

Upregulated SK2 Expression and Impaired CaMKII Phosphorylation Are Shared Synaptic Defects Between 16p11.2del and 129S: Δ disc1 Mutant Mice

Razia Sultana¹, Tanya Ghandi¹, Alexandra M. Davila¹, Charles C. Lee¹, and Olalekan M. Ogundele¹ 

ASN Neuro
Volume 10: 1–14
© The Author(s) 2018
Article reuse guidelines:
sagepub.com/journals-permissions
DOI: 10.1177/1759091418817641
journals.sagepub.com/home/asn


Abstract

Ion channel gating and kinase regulation of N-methyl-D-aspartate receptor 1 activity are fundamental mechanisms that govern synaptic plasticity. In this study, we showed that two mutant models (16p11.2del and Δ disc1) that recapitulate aspects of human cognitive disorders shared a similar defect in N-methyl-D-aspartate receptor 1-dependent synaptic function. Our results demonstrate that the expression of small-conductance potassium channels (SK2 or KCa2.2) was significantly upregulated in the hippocampus and prefrontal cortex of 16p11.2del and 129S: Δ disc1 mutant mice. Likewise, both mutant strains exhibited an impairment of T286 phosphorylation of calcium-calmodulin-dependent kinase II (CaMKII) in the hippocampus and prefrontal cortex. *In vivo* neural recordings revealed that increased SK2 expression and impaired T286 phosphorylation of CaMKII coincide with a prolonged interspike interval in the hippocampal cornu ammonis-1 (CA1) field for both 16p11.2del and 129S: Δ disc1 mutant mice. These findings suggest that alteration of small conductance channels and T286 phosphorylation of CaMKII are likely shared factors underlying behavioral changes in these two genetic mouse models.

Keywords

16p11.2del, Δ disc1, SK2, CaMKII, neural encoding, cognition

Received July 30, 2018; Received revised November 7, 2018; Accepted for publication November 9, 2018

Introduction

Neuropsychiatric disorders are characterized by changes in synaptic structure and composition of synapses in parts of the brain associated with cognitive function (Pezes et al., 2011; Gonzalez Burgos et al., 2012; Borrie et al., 2017; Reim and Schmeisser, 2017). Such changes may result from genetic mutation (Corriveau et al., 1998; West et al., 2001), modifications to protein–substrate interaction (Loving et al., 1986; Morishita et al., 2001), and deformity of synaptic structure proteins (Shapiro and Eichenbaum, 1999; Chechlacz and Gleeson, 2003; Anticevic et al., 2012). Together, these changes result in synaptic dysfunction and are underlying causes of the abnormal behavioral patterns that is observable in the affected individual.

In the hippocampus and prefrontal cortex (PFC), synaptic long-term potentiation (LTP) is modulated by N-methyl-D-aspartate receptor 1 (NMDAR) activation

(Li et al., 2001; Salter and Kalia, 2004), which is regulated, in part, by ion movement and synaptic kinase molecular switch systems (Giese et al., 1998; Gao and Zhao, 2018; Incontro et al., 2018). NMDAR signaling, through increased Ca²⁺ current, couples synaptic potentiation to cellular regulation by promoting the phosphorylation of downstream kinases (Borrie et al., 2017; Reim and Schmeisser, 2017). However, NMDAR potentiation in glutamatergic neurotransmission and accompanying Ca²⁺ flux are not isolated events during LTP. Tuning

¹Department of Comparative Biomedical Sciences, Louisiana State University School of Veterinary Medicine, Baton Rouge, LA, USA

Corresponding Author:

Olalekan M. Ogundele, Department of Comparative Biomedical Sciences, Louisiana State University School of Veterinary Medicine, Baton Rouge, LA 70803, USA.

Email: ogundele@lsu.edu



of NMDAR-mediated Ca^{2+} current by small-conductance potassium channels (SK2 or $\text{KCa}_{2.2}$) constitutes an ion channel gating mechanism of synaptic potentiation. SK2 is activated by Ca^{2+} currents generated by the GluN1 subunit of NMDAR during synaptic potentiation. Since SK2 channels are activated by GluN1-mediated Ca^{2+} currents, an increase in synaptic potentiation will equally increase SK2 activity and K^+ efflux (Hammond et al., 2006; Allen et al., 2007; Lin et al., 2008; Allen et al., 2011). Together, synaptic potentiation embodies the movement of ions in organized events of oscillation between Ca^{2+} and K^+ currents (Hammond et al., 2006; Allen et al., 2011). Previous studies have shown that the efficiency of this process is altered in some neuropsychiatric disorders (Decker et al., 2010; Dibue et al., 2013; Dibue-Adjei et al., 2017; Nakazawa et al., 2017).

In synaptic potentiation, elevated levels of Ca^{++} has been shown to initiate biochemical cascade through activation of synaptic regulatory calcium-calmodulin-dependent kinase II alpha ($\text{CaMKII}\alpha$; Lisman et al., 2002, 2012). This is major synaptic protein that is structurally linked with the GluN2B subunit of NMDAR (Coultrap and Bayer, 2012; Coultrap et al., 2014). When activated by Ca^{++} currents, autophosphorylation of the Thr286 site and increased Ca^{++} -calmodulin (CaM) binding represent significant steps in LTP (Coultrap and Bayer, 2012; Lisman et al., 2012). Although NMDAR hypofunction has been described in some cognitive disorders (Gandal et al., 2012; Snyder and Gao, 2013; Cohen et al., 2015), recent work also suggest that genetic ablation of CaMKII can lead to synaptic and behavioral symptoms of developmental disorders (Yamasaki et al., 2008; Matsuo et al., 2009). Because GluN1-mediated Ca^{++} currents activates SK2 channels, which in turn decrease the threshold and frequency of action potentials, there is a rationale to test whether hyperactivity of SK2 channels can mediate NMDAR hypofunction by blocking CaMKII activation. In a previous study, we described a possible relationship between CaMKII and SK2 activity in a model of developmental neuropsychiatric disorder that recapitulate NMDAR hypofunction. We noted an inverse relationship for the expression of CaMKII and SK2 on dendritic spines in the hippocampal cornu ammonis-1 (CA1) region of mice (Figure 1). As such, after induction of NMDAR hypofunction, CA1 neurons exhibited significant loss of CaMKII , increased SK2 expression, and increased K^+ leak current (Ogundele and Lee, 2018).

NMDAR hypofunction (Snyder and Gao, 2013; Lee et al., 2015) has been reported previously in genetic mutations that recapitulates some of the symptoms of developmental neurocognitive defects. Specifically, microdeletion of 16p11.2del has been shown to cause some of the behavioral defects associated with autism,

while its duplication has been linked with schizophrenia (Horev et al., 2011). Likewise, mutation of the *disc1* gene has been shown to cause a truncation of the structure of a synaptic protein—*disc1* (Kvajo et al., 2008). While 16p11.2del is broadly associated with a defective Erk1/2 signaling, *disc1* mutation is linked to a defective neural GSK3 β signaling (Mao et al., 2009; Pucilowska et al., 2015). Interestingly, both mutations have demonstrated a significant similarity in synaptic pathophysiology as indicated by a significant loss of NMDAR function (Halene et al., 2009; Gandal et al., 2012). However, till date, how these mutations might have impacted the expression of SK2 and CaMKII and their significance in the propagation of NMDAR hypofunction remains relatively unclear. Here, we investigated the relationship between SK2 expression and CaMKII Thr286 phosphorylation in the hippocampus and PFC of genetic mutant mice—16p11.2del and Δdisc1 mice—previously characterized by NMDAR hypofunction. Similar to pharmacologically induced NMDAR hypofunction (Ogundele and Lee, 2018), our results demonstrate an overexpression of SK2 in the hippocampus and PFC of 16p11.2del and Δdisc1 mutant mice. In addition, both mutant models exhibited a defective T286 phosphorylation of CaMKII in the hippocampus and PFC.

Methods

Animals

Adult male (PND90-100) 16p11.2del (RRID: IMSR_JAX:01312) and Δdisc1 mutant (RRID: IMSR_JAX:002448) mice were acquired from The Jackson Laboratory (Bar Harbor, ME, USA). Both 16p11.2del and Δdisc1 mutant mice were bred on a 129S background and are characterized by NMDAR hypofunction in the cognitive centers. These mutant models are particularly suitable for studying aspects of synaptic and behavioral defects of autism (16p11.2del) and schizophrenia (Δdisc1). It is important to note that a broad range of other developmental synaptic defects may also be present in mice carrying these mutations. Generally, both 16p11.2del and Δdisc1 mice exhibit a significant decline in sociocognitive function. We used wild-type C57BL/6J mice (RRID:IMSR_JAX:000664) as controls because the 129S mouse line is prone to spontaneous mutation of the *disc1* gene. Both mutant mouse lines (i.e., 16p11.2del and 129S: Δdisc1) have been characterized previously for the respective mutations and neurocognitive defects (Kvajo et al., 2008; Horev et al., 2011; Pucilowska et al., 2015; Dittrich et al., 2017). Animals were housed under standard laboratory condition of 12-hr alternating light and dark cycle, with food and water provided ad libitum. All animal handling procedures were approved by the Institutional Animal Care

and Use Committee of the Louisiana State University. Animals used for this study weighed between 22 and 26 g.

In Vivo Electrophysiology Recording

We conducted *in vivo* electrophysiological recordings in anesthetized mice. Animals were deeply anesthetized with urethane (0.2 mg/kg ip); then, the head was affixed on a stereotaxic frame. A toe pinch test was performed to ensure the absence of pain sensation before the commencement of the procedure. A 7 × 7-mm skull area was removed using a drill bit (Dremel) to expose the dura. Drops of artificial cerebrospinal fluid were applied to this area to prevent dryness. Under a digital dissection microscope, the dura over the exposed area was carefully excised using a bent needle tip. An acute neural probe, with a 10-mm long and 50- μ m thick shank, was used for this procedure (Neuronexus, MI, USA). The probe shank carried four electrodes arranged as a tetrode, with an interelectrode distance of 25 μ m. The electrodes were connected to a 32-channel preamplifier head stage (Intantech, CA, USA), linked to a 512-channel recording controller and amplifier system (Intantech). The electrode was gently lowered into the brain tissue using an ultrafine (μ m range) hydraulic micromanipulator (Narishige, Japan) to reach the CA1- dentate gyrus (DG) field at stereotaxic coordinates (AP: +2.2 mm, ML: +2.0 mm, DV: +1.78 mm) relative to the Bregma. Stainless steel ground wires soldered onto the head stage-electrode adapter (Neuronexus; A4 to Omnetics CM32 adapter) were tied to a ground screw that was fixed in the occipital bone.

The stereotaxic apparatus, micromanipulator, electrode, and subject mouse were housed in a Faraday cage and were grounded to the recording controller amplifier unit. To ensure proper grounding, we assessed root mean square values (ranged between 3.2 and 5.0 μ V) and checked baseline local field potential (0.1 Hz–200 Hz) for electrical noise (60 Hz). At the onset of each rerecording procedure, we tested the impedance of the electrodes at 1000 Hz. For all recordings, impedance measurement for the silicon tetrodes ranged between 0.6 and 3.1 meg Ω . Single unit activity was recorded by setting on-chip digital signal processing (DSP) filter frequency (0.1 Hz), lower cutoff frequency (0.1 Hz), and an upper cutoff frequency (20000 Hz) in the recording controller software interface. Single-unit activity was monitored for 20 min to ensure the stability of the animal's vitals and electrode channel activity. Subsequently, we recorded the data continuously for 30 min. Acquired neural recordings from the CA1-DG field (continuous data) were processed in an Offline Spike Sorting software (Version 4.4.0; Plexon Inc., Dallas, TX, USA; RRID:SCR_000012). Further analysis of the sorted spikes was done in

NeuroExplorer Version 5.121 (Nex Technologies, Fairfax, VA, USA; RRID:SCR_001818).

Neural Spike Processing and Analysis

Neural spikes were extracted from the continuous data through threshold crossing in the OFSS. The extracted spikes were sorted using an unsupervised valley-seeking method and clustering in three-dimensional (3-D) PCA space. Where necessary, unsorted spikes were assigned to clustered units, or invalidated if outlying. Sorted neural spike waveforms, clustered units, and continuous data were exported into the NeuroExplorer software for further analysis. Continuously recorded data from at least two electrode units were considered per mice. In the NeuroExplorer platform, autocorrelogram and inter-spike interval (ISI) histograms were plotted for the sorted spikes.

Immunoblotting

Deeply anesthetized mice were euthanized in an isoflurane chamber. The animals were transcardially perfused with 10 mM phosphate-buffered saline (PBS; pH 7.4), and the whole brain was removed. The harvested brain was rapidly placed in cold artificial cerebrospinal fluid maintained on ice and saturated with 95% oxygen/5% CO₂. A clean razor blade was used to cut the brain—along the sagittal plane—into two (left and right) hemispheres. In both hemispheres, the hippocampus was microdissected, then extracted by exposing the space between the sensory cortex (above), and corpus callosum (below). Subsequently, a surgical blade was used to trim the left PFC. The harvested hippocampal and prefrontal cortical tissue were kept in separate tubes and stored at –80°C until further use.

Frozen hippocampal and prefrontal cortical tissue were incubated on ice with radioimmunoprecipitation assay lysis cocktail containing protease and phosphatases inhibitors. After 30 min, the incubated tissue was rapidly homogenized to obtain tissue lysate. We centrifuged the homogenate to obtain supernatants containing cytoplasmic, membrane, and synaptic fragments.

Then, 10 μ l hippocampal lysate containing 10 μ g of protein was processed for sodium dodecyl sulphate-polyacrylamide gel electrophoresis. After Western blotting (wet transfer), the polyvinylidene fluoride membrane was incubated in Tris-buffered saline (with 0.01% Tween 20) for 15 min (TBST) at room temperature. Afterward, the membrane was blocked in 3% bovine serum albumin (prepared in TBST) for 50 min at room temperature. The protein of interest and housekeeping protein were detected using the following primary antibodies; rabbit anti-SK2 antibody (ThermoFisher Scientific, Waltham, MA, US. #PA5-41071; RRID:AB_2605451); mouse

anti-CaMKII α antibody (ThermoFisher Scientific #MA1-048; RRID:AB_325403), rabbit anti-Phospho-CaMKII α : T286, and (Cell Signaling, Waltham, MA, US. #12716; RRID:AB_2713889), rabbit anti-NMDAR1:GluN1 polyclonal antibody (ThermoFisher Scientific #PA3-102; RRID:AB_2112003). All primary antibodies were diluted in the blocking solution at 1:1,000. Subsequently, the primary antibodies were detected using chicken anti-rabbit-HRP (ThermoFisher Scientific #A15987; RRID:AB_2534661) or donkey anti-mouse-HRP (ThermoFisher Scientific #A16017; RRID:AB_2534691) secondary antibody, at a dilution of 1:5,000 or 1:10,000. The reaction was developed using a chemiluminescence substrate (ThermoFisher Scientific #34579). To normalize protein expression, the membranes were treated with Restore PLUS Western Blot Stripping Buffer (ThermoFisher Scientific #46430) and reprobed with β -actin (8H10D10) mouse mAb HRP conjugate (Cell Signaling #12262S).

Immunofluorescence

The brain was fixed in 4% phosphate-buffered paraformaldehyde overnight at room temperature and then transferred to 4% phosphate-buffered paraformaldehyde containing 30% sucrose for cryopreservation at 4°C. Free-floating cryostat sections (20 μ m) were obtained and preserved in 48-well plates containing 10 mM PBS at 4°C (WT-control: $n = 5$, 16p11.2del: $n = 5$; Δ disc1: $n = 6$). The sections were washed three times (5 min each) in 10 mM PBS (pH 7.4) on a slow orbital shaker. Subsequently, nonspecific blocking was performed in normal 5% normal goat serum (Vector Labs, Malvern, PA, US. #S-1000; RRID:AB_2336615), prepared in 10 mM PBS + 0.03% Triton-X100, for 1 hr at room temperature. The sections were incubated overnight at 4°C in primary antibody—rabbit anti-SK2 antibody (ThermoFisher Scientific #PA5-41071)—diluted in blocking solution (10 mM PBS + 0.03% Triton-X 100 and 5% normal goat serum). Subsequently, the sections were washed two times in 10 mM PBS and incubated in a secondary antibody—goat anti-rabbit Alexa 488 (ThermoFisher Scientific #A-11034; RRID:AB_2576217)—diluted in the blocking solution. Secondary antibody incubation was done for 1 hr at room temperature, with gentle shaking (35 rpm). Immunolabeled sections were washed and mounted on gelatin-coated slides using ProLong™ Diamond Antifade Mountant (ThermoFisher Scientific #P36970).

Quantification

Fluorescence imaging was performed using a Nikon-NiU fluorescence upright microscope configured for 3-D

imaging. Z-stacks were obtained across a depth of 15 μ m and converted into 2-D images through the extended depth of focus (EDF) option on Nikon Element Advanced Research software (RRID:SCR_014329). Normalized fluorescence intensity for immunolabeled proteins in the hippocampus and medial PFC was determined in optical slices for serial section images ($n = 5$). Fluorescence intensity was quantified using Nikon Element AR. Mean cell count and intensity were determined per μ m² for $n = 12$ areas in several fields of view for consecutive sections. Fluorescence intensity was normalized by applying a uniform exposure time for a fluorophore-labeled protein in experimental and control brain slices.

Immunoblots

The expression of SK2, CaMKII, and GluN1 was normalized *per lane* using the corresponding β -actin expression. However, T286 pCaMKII was normalized by the corresponding CaMKII expression for each sample.

Statistical Analysis

Statistical comparison between WT, 16p11.2del and 129S: Δ disc1 protein expression, fluorescence intensity, time spent in sociability chamber, and neural activity was determined using one-way analysis of variance with Mann–Whitney post hoc test. This was computed in GraphPad Prism version 7.0 (RRID:SCR_002798). Here, we presented the results as bar graphs with error bars depicting the mean and standard error of mean, respectively, for all bar graphs.

Results

SK2

Our results showed that SK2 expression was significantly upregulated in the hippocampus and PFC of 16p11.2del and 129S: Δ disc1 mutant mice. Immunoblot analysis of hippocampal extracts demonstrates a prominent increase in SK2 expression for 16p11.2del ($p < .01$) and 129S: Δ disc1 ($p < .05$) mutant mice when compared with controls (Figure 2(a) and (b)). This outcome was consistent with immunofluorescent labeling for SK2. Here, we compared normalized fluorescence intensity for SK2 that is colocalized with NeUN/DAPI in the CA1 of control and mutant mice. There was an increased labeling intensity of SK2 in the CA1 for 16p11.2del ($p < .05$) and 129S: Δ disc1 ($p < .01$) mutant hippocampus when compared with controls (Figure 2(c) and (d)).

Similarly, immunoblot analysis of tissue extracts from PFC revealed a significant increase in SK2 expression for 16p11.2del ($p < .01$) and 129S: Δ disc1 mutant mice ($p < .01$) versus controls (Figure 2(e) and (f)).

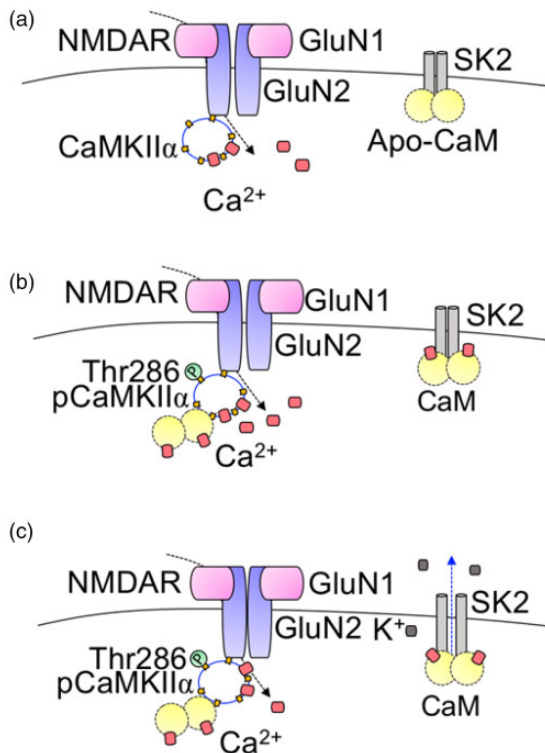


Figure 1. Schematic illustration of the possible mechanism of CaMKII regulation of NMDAR and SK2. (a) CaMKII α is bound to the GluN2 subunit of NMDAR. Likewise, calmodulin (ApoCaM) is constitutively bound to SK2 around the pore-forming loop. (b) Activation of NMDAR by glutamate binding increases Ca²⁺ influx which promotes T286 phosphorylation of CaMKII α . Phospho (T286) CaMKII has increased affinity for CaM binding. (c) During high-frequency synaptic potentiation, there is a repetitive activation of SK2 which facilitates K⁺ efflux that contributes to the termination of the synaptic potentiation event. NMDAR = N-methyl-D-aspartate receptor 1; SK2 = small-conductance potassium channels; CaMKII α = calcium-calmodulin-dependent kinase II.

Normalized fluorescence intensity for SK2 that is colocalized with NeUN/DAPI also increased significantly in medial PFC sections of 16p11.2del ($p < .01$) and 129S:Δdisc1 ($p < .01$) mutant mice when compared with the controls (Figure 2(g) and (h)).

CaMKII α Expression and T286 Phosphorylation

In prior work, we showed that pharmacological inhibition of NMDAR was associated with a significant upregulation of SK2 expression and loss of CaMKII in the hippocampal CA1 region of mice (Ogundele and Lee, 2018). The results of this study suggest a similar expression pattern for CaMKII and SK2 in the hippocampus and PFCs of 16p11.2del and 129S:Δdisc1 mutant mice. Immunoblot analysis of hippocampal tissue extracts reveals a significant decrease in neural CaMKII—normalized with β -actin—expression in mice carrying

16p11.2del ($p < .05$) and 129S:Δdisc1 mutation ($p < .05$) versus the controls (Figure 3(a) and (b)). Furthermore, both mutant strains exhibited significant impairments in T286 phosphorylation of CaMKII when compared with the controls. As such, T286-phosphorylated CaMKII—phospho (T286) CaMKII—normalized with CaMKII—was significantly downregulated in the hippocampus of 16p11.2del ($p < .001$) and 129S:Δdisc1 mutant mice ($p < .001$) when compared with the control (Figure 3(a) to (c)). Like the hippocampus, both 16p11.2del ($p < .01$) and 129S:Δdisc1 mutant mice ($p < .01$) exhibited a significant loss of prefrontal cortical CaMKII expression versus the controls (Figure 3(d) and (e)). Furthermore, T286 phosphorylation of CaMKII in the PFC was also impaired for both mutant strains—16p11.2del ($p < .001$) and 129S:Δdisc1 mutant ($p < .001$)—when compared with the controls (Figure 3(d) and (f)).

NMDAR-GluN1

A significant part of the synaptic and cognitive deficits associated with 16p11.2del and 129S:Δdisc1 mutation has been linked to a change in the expression or activity of NMDAR. Our results show that the expression of the GluN1 subunit of NMDAR was significantly upregulated in the hippocampus of 16p11.2del mice when compared with controls (Figure 4(a) and (b); $p < .05$). However, no significant change was observed for hippocampal NMDAR-GluN1 expression in 129S:Δdisc1 mutant mice versus the controls. Similar to our observation in the hippocampus of 16p11.2del mice, the PFC also exhibited a prominent increase in NMDAR-GluN1 expression when compared with controls ($p < .05$; Figure 4(c) and (d)). Furthermore, there was a significant increase in prefrontal cortical NMDAR-GluN1 expression for 129S:Δdisc1. Although NMDAR hypofunction has been described for the associated behavioral changes in mice carrying these mutations, our results show that the expression of NMDAR did not decrease when compared with the control. However, NMDAR hypofunction may have been induced by an increased SK2 expression (and activity) and defective T286 phosphorylation of CaMKII.

Bursting Activity

To evaluate the significance of synaptic changes in the PFC–hippocampus circuit, we assessed the synchronization of spontaneously evoked neural activity in the CA1-DG field, which receives significant inputs from PFC (Parent et al., 2010; Godsil et al., 2013). Figure 5(a) illustrates the arrangement of electrodes on the shank of the silicon neural probe. Spikes extracted from the continuous data through threshold crossing were sorted into single-unit clusters in a 3-D PCA space (Figure 5(b) and (c)). After spike sorting, the continuous data were aligned with rasters

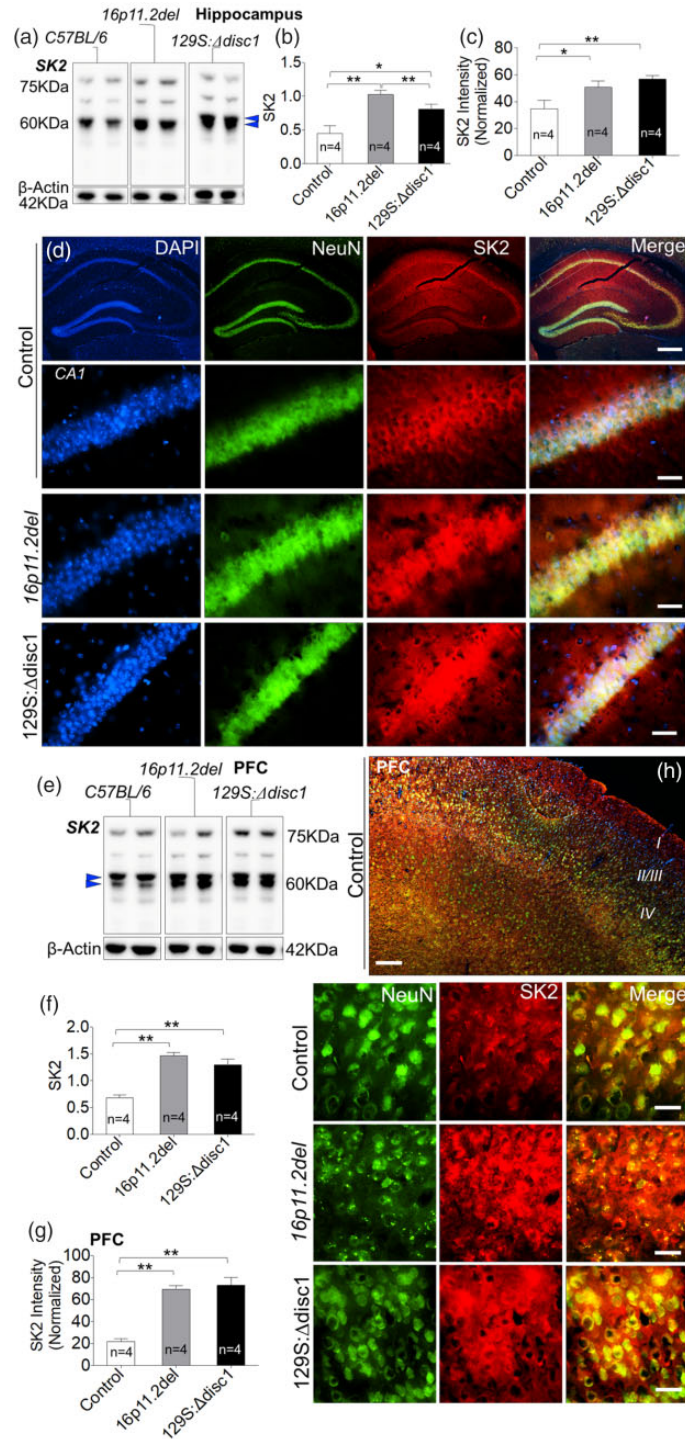


Figure 2. SK2 expression is upregulated significantly in the hippocampus and PFC of 16p11.2del and 129S: Δ disc1 mutant mice. (a and b) Immunoblots and bar graph depicting a significant increase in hippocampal SK2 expression for 16p11.2del ($p < .01$) and 129S: Δ disc1 mutant ($p < .01$) mice when compared with the control. Blue arrow head in (a) indicates quantified bands (60–66 KDa). (c and d) Bar graph and representative fluorescence images illustrating an increase in normalized intensity of SK2 in the hippocampal CA1 region of 16p11.2del ($p < .05$) and 129S: Δ disc1 mutant ($p < .01$) mice versus the control. Scale bar: 100 μ m (c) (scale bar: 100 μ m and 20 μ m). (e and f) Immunoblots and bar graphs demonstrating an increased SK2 expression in the PFC of 16p11.2del ($p < .01$) and 129S: Δ disc1 mutant mice ($p < .01$). Blue arrow head in (e) indicates quantified bands (60–66 KDa). (g and h) Bar graph and fluorescence images depicting a significant increase in SK2 intensity in the mPFC of 16p11.2del mice ($p < .01$) and 129S: Δ disc1 mutant mice ($p < .01$) when compared with the control (scale bar: 100 μ m and 20 μ m). SK2 = small-conductance potassium channels; PFC = prefrontal cortex.

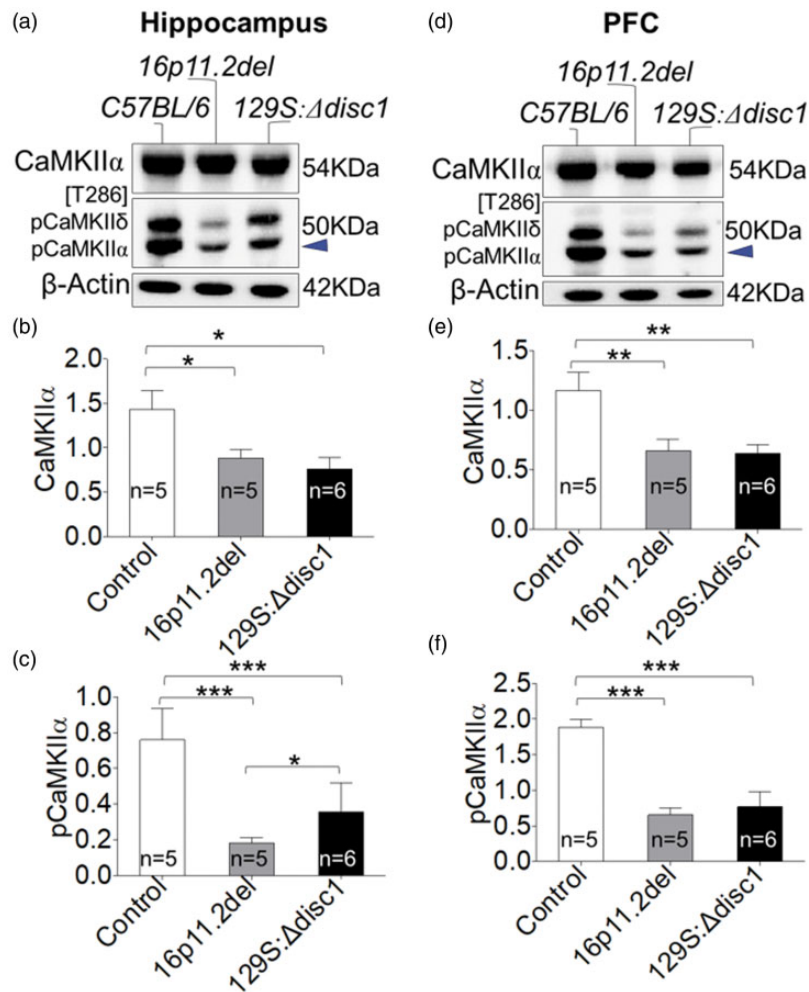


Figure 3. Reduced CaMKII α expression and impaired T286 phosphorylation in the hippocampus and PFC of 16p11.2del and 129S: Δ disc1 mutant mice. (a) Representative Western blots and bar graph showing a significant decrease in the expression of CaMKII α - and T286-phosphorylated CaMKII α in the hippocampus of 16p11.2del and 129S: Δ disc1 mutant mice. Blue arrow head in (a) indicates quantified band (50KDa; pCaMKII α). (b) Bar graph showing a significant decrease in hippocampal CaMKII α expression for 16p11.2del ($p < .05$) and 129S: Δ disc1 mutant mice ($p < .05$) versus the control. (c) Bar graph depicting a significant decrease in T286-phosphorylated CaMKII α in the hippocampus of 16p11.2del mice ($p < .001$) and 129S: Δ disc1 mutant mice ($p < .001$) when compared with the control. (d) Representative immunoblots demonstrating a significant loss of prefrontal cortical CaMKII α - and T286-phosphorylated CaMKII α for 16p11.2del and 129S: Δ disc1 mutant mice. (e) Bar graph depicting a significant decrease in prefrontal cortical CaMKII α expression for 16p11.2del ($p < .01$) and 129S: Δ disc1 mutant mice ($p < .01$) when compared with the control. (f) Bar graph showing a decreased expression of T286-phosphorylated CaMKII α in the PFC of 16p11.2del ($p < .001$) and 129S: Δ disc1 mutant mice ($p < .001$) when compared with the control. PFC = prefrontal cortex; CaMKII = calcium-calmodulin-dependent kinase II.

for each neuron units, by time segments (Figure 5(d) to (f)). Subsequent analysis of spiking frequency (raster ticks) revealed a significant decrease in spontaneously evoked CA1 neural spikes for 16p11.2del ($p < .001$) and 129S: Δ disc1 mutant ($p < .01$) versus controls (Figure 5(g)).

When we examined the temporal firing pattern for neuron 1 (n1) and neuron 2 (n2) in a single spike train, n1 and n2 spikes were mostly out of phase in 16p11.2del and 129S: Δ disc1 mutant neurons. This was evident when a burst (2–3 spikes/s) in either the n1 or n2 spike train was chosen as the reference

time t_0 event (Figure 5(d) to (f)). We further evaluated the aligned rasters and then manually matched rasters for n1 and n2. Rasters in the control spike train revealed a significantly higher number of bursts per unit time (50 ms) when compared with 16p11.2del and 129S: Δ disc1 mutant mice (Figure 5(h); $p < .001$). In addition, there was a significant desynchronization in the firing pattern for an n1/n2 pair in 16p11.2del and 129S: Δ disc1 mutant CA1-DG field. When the neuron with the higher activity (spikes/s) was chosen as the reference event, neurons from mutant mice

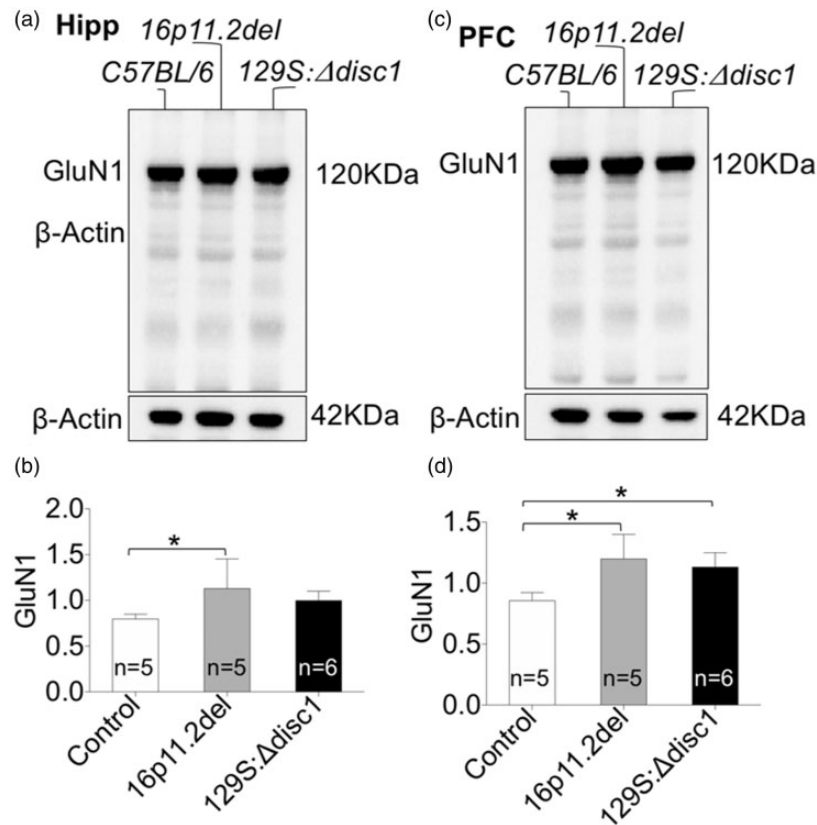


Figure 4. GluN1 expression in the hippocampus and prefrontal cortex of 16p11.2del and 129S:Δdisc1 mutant mice. (a and b) Immunoblots and bar graph showing an increased expression of the GluN1 in the hippocampus of 16p11.2del ($p < .05$)—and not 129S:Δdisc1 mutant mice—when compared with the control. (c and d) Immunoblots and bar graph showing an increased expression of GluN1 in the PFC of 16p11.2del ($p < .05$) and 129S:Δdisc1 mutant mice ($p < .05$) versus the control. PFC = prefrontal cortex.

exhibited a decrease in the number of correct trials (Figure 5(i); 16p11.2del: $p < .01$ and 129S:Δdisc1: $p < .01$) when compared with controls. Furthermore, there was a significant increase in percentage error per trial for the mutant hippocampus (Figure 5(j); 16p11.2del: $p < .05$ and 129S:Δdisc1: $p < .01$) versus the control.

Refractory Period and the Significance of Upregulated SK2 Expression

In immunoblot analysis, our results demonstrate increased neural expression of SK2 in the hippocampus and PFC of 16p11.2del and 129S:Δdisc1 mutant mice (Figure 2). To adequately ascertain whether a change in SK2 expression was accompanied by increased SK2 activity, we measured neural refractoriness in the form of the ISI, which corresponds to the opening of K^+ channels during the after-hyperpolarization phase of a synaptic potential. Controls exhibited a rapid ISI with a peak strength of 30 spikes/s. The peak strength reduced rapidly for successive firing (bursts; Figure 6(a) and (b)). However, in 16p11.2del mice, there was a

significant reduction in the ISI histogram peak strength (10 spikes/s) when compared with the control (Figure 6 (b); $p < .01$). Furthermore, the decay periods of the ISI histogram did not return to full resting potential, unlike the control (Figure 6(a); label *i*). Similarly, in 129S:Δdisc1 mutant mice, there was a significant decrease in ISI peak strength (15 spikes/s) versus the control ($p < .01$; Figure 6 (a) and (b)). Although there were intermittent decay periods, these intervals did not return to zero points in between peaks (Figure 6(a); label *i*).

In addition to a weak ISI peak for 16p11.2del and 129S:Δdisc1 mutant CA1-DG field, we also recorded a prolonged ISI in these mice. As illustrated by black arrowheads in the ISI histogram (Figure 6(a)), 16p11.2del and 129S:Δdisc1 mutant neurons recorded ISI at t_0 ms, which suggests a prolonged ISI for events at t_0-1 ms. Thus, the time interval between t_0 and the successive ISI peak was significantly reduced for 16p11.2del ($p < .001$) and 129S:Δdisc1 mutant ($p < .001$) neurons versus the controls (Figure 6(a) and (c)). When we plotted the peak of successive ISI histograms against time (from 0 ms to 500 ms), it was noted that the control

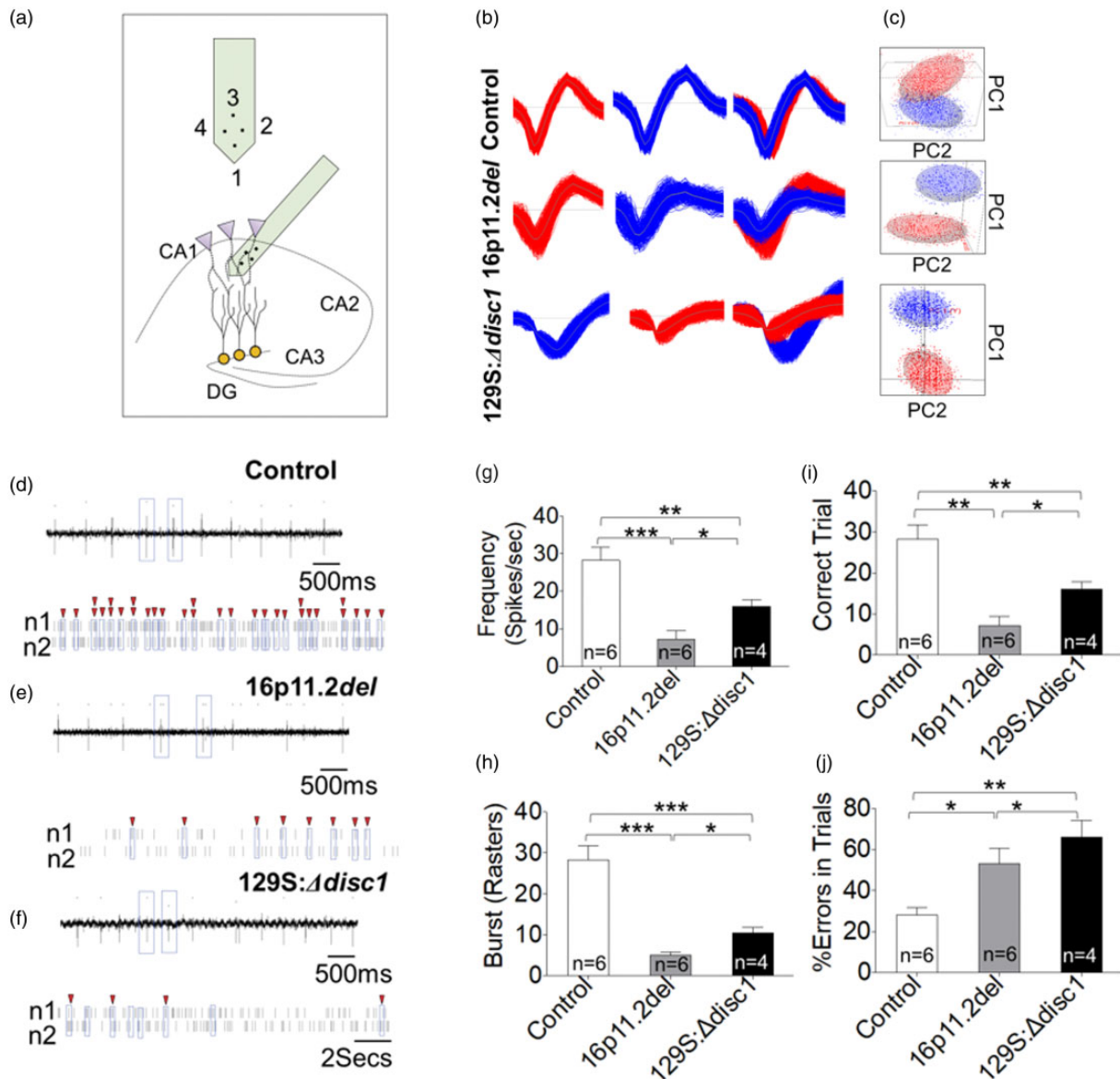


Figure 5. In vivo physiological recordings from the hippocampal CA1-DG field. (a) Schematic illustration of the electrode design and relative positioning of the electrode units in the CA1-DG field. (b) Neural spike waveform extracted from continuous data recorded through single electrode channel in anesthetized mice. (c) PCA projections and clustering of the sorted spikes in the CA1-DG field of the hippocampus. (d-f) Continuous recording with aligned rasters. The neuron with the higher spike count was used as the reference event, and the first burst was used as the start time for analysis (n1: neuron 1, n2: neuron 2). (g) Bar graph showing a one-way analysis of variance comparison for the spiking frequency (spikes/s). 16p11.2del ($p < .001$) and 129S:Δdisc1 mutant mice ($p < .01$) recorded a decrease in frequency of spontaneously generated CA1 spiking activity when compared with the control. (h) Bar graph demonstrating the comparative distribution of spike bursts in the action potential train for 16p11.2del ($p < .001$) and 129S:Δdisc1 mutant neurons ($p < .001$) when compared with the control. (i) Bar graph showing a significant decrease in correct trials for single unit activity in the CA1-DG field of 16p11.2del ($p < .01$) and 129S:Δdisc1 mutant mice ($p < .01$) versus the control. (j) 16p11.2del ($p < .05$) and 129S:Δdisc1 mutant ($p < .01$) neural activity was also characterized by prominent desynchronization. This was seen as an increased percentage error per trial when compared with the control.

ISI peaks reached resting potential (0 ISI/s) by 200 ms. Conversely, both 16p11.2del and 129S:Δdisc1 mutant recorded peaks above 0 ISI/s after the 500-ms mark. This is illustrated as a red arrowhead in Figure 6(d).

Discussion

In this study, we examined both SK2 and CaMKII regulation of NMDAR in the hippocampus and PFC of 16p11.2del and 129S:Δdisc1 mutant mice. The rationale

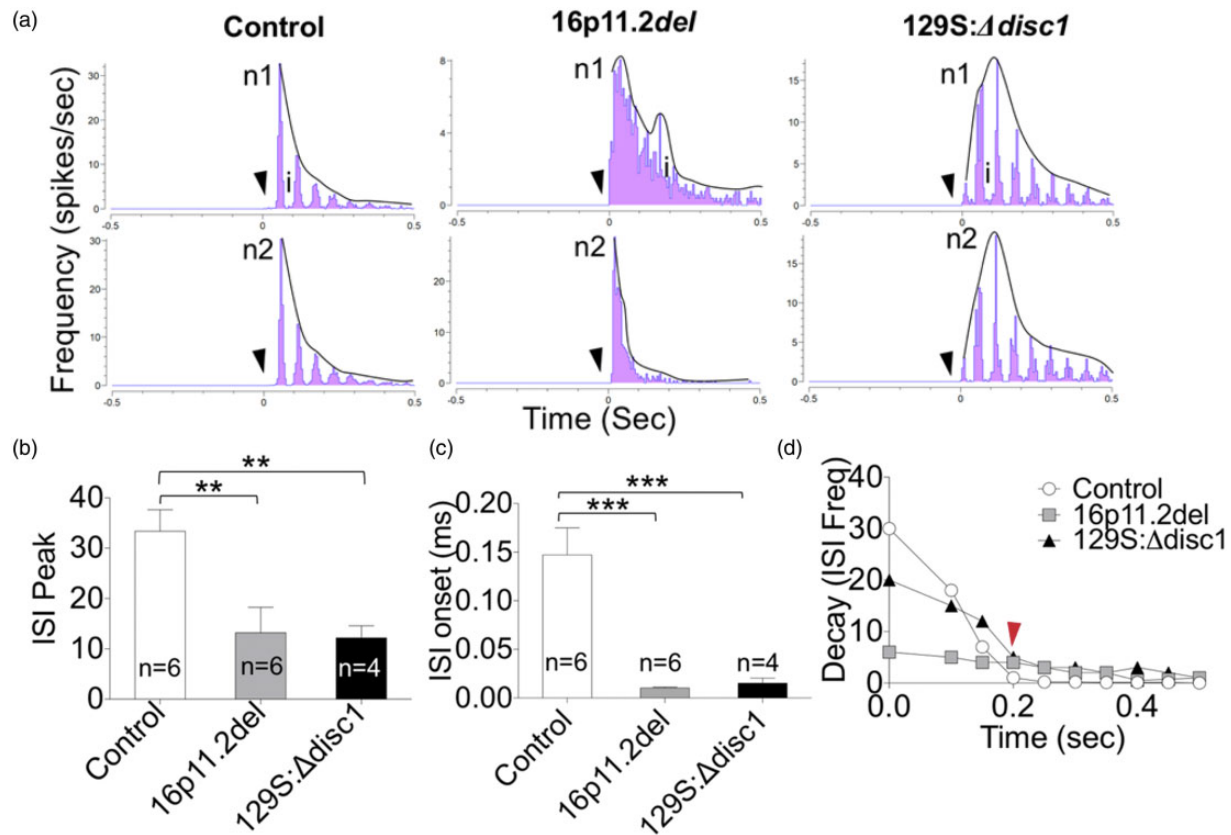


Figure 6. ISI as a measure of SK2 activity and trapping of CaM by T286 phospho (T286) CaMKII. (a) Neural activity recorded from 16p11.2del and 129S:Δdisc1 mutant CA1-DG field was characterized by a significant increase in the ISI. (b) Bar graph showing a reduction in ISI peak reduced for 16p11.2del ($p < .01$) and 129S:Δdisc1 mutant neural activity ($p < .01$) when compared with the control. (c) Bar graph depicting a rapid onset (at $t = 0$) for ISI in 16p11.2del and 129S:Δdisc1 mutant neural activity (black arrowheads). As such, the onset for an ISI event (in $t = \text{ms}$) was significantly reduced in 16p11.2del and 129S:Δdisc1 mutant neural activity ($p < .001$ versus the control). (d) Correlation plot showing a prolonged decay period for the ISI in mutant CA1-DG neural activity. The control showed a rapid onset (peak) and decay of ISI (200 ms). Conversely, 16p11.2del and 129S:Δdisc1 neural activities were characterized by a prolonged duration of ISI events (>500 ms); depicted a red arrow. ISI = interspike interval.

for this study arose from our prior work in which we pharmacologically induced synaptic changes previously described in some developmental neuropsychiatric disorders (Ogundele and Lee, 2018). There, we demonstrated a significant upregulation of SK2 and loss of CaMKII in the hippocampal CA1 region of behaviorally deficient mice, after an induced NMDAR hypofunction. This was particularly interesting as hippocampal neurons in these mice also showed a prolonged after-hyperpolarization phase when assessed through whole-cell patch clamp recording (Ogundele and Lee, 2018). This led us to ask whether SK2 expression and function may be altered in genetic mutations that are broadly characterized by cognitive defects and alterations in NMDAR function.

Previous studies have identified synaptic changes for both the 16p11.2 copy number variation (microdeletion) and the Δdisc1 mutation (Kvajo et al., 2008; Horev et al.,

2011; Wang et al., 2011; Pucilowska et al., 2015). In the human population, Δdisc1 mutations and microdeletions of 16p11.2 gene locus have been identified as predisposing factors to complex neuropsychiatric disorders, such as schizophrenia and autism, respectively (Kvajo et al., 2008; Horev et al., 2011). Among other defects, impairment of LTP, neurotransmitter imbalance, abnormal protein expression (Brandon et al., 2009; Pucilowska et al., 2015), and defective glutamatergic neurotransmission have been described for these mutations (Tropea et al., 2016; Crabtree et al., 2017).

Normal NMDAR expression and activity at postsynaptic densities underlie synaptic LTP and plasticity. As such, changes in the expression or activity of NMDAR can alter dendritic spine structure (Penzes et al., 2011; Gonzalez Burgos et al., 2012; Stein et al., 2015). The regulation of NMDAR activity is particularly important

in hippocampal and prefrontal cortical synapses concerned with cognitive function. While the hippocampus is responsible for the transient organization of cortical inputs (Eichenbaum, 2000), with organized hippocampal–cortical outputs (Cutsuridis et al., 2010; Ratnadurai-Giridharan et al., 2014), the efficiency of this process is dependent on the tuning of NMDAR activity through ionotropic and synaptic kinase interactions. Impairment of such regulatory processes may promulgate cognitive and behavioral defects (Morishita et al., 2001; Salter and Kalia, 2004; Gao et al., 2018).

SK2 and NMDAR are colocalized at postsynaptic densities. Together with α -amino-3-hydroxy-5-methyl-4-isoxazolepropionic acid receptor (AMPA) receptors, SK2 regulates the excitability of NMDAR during synaptic potentiation (Hammond et al., 2006; Lin et al., 2008; Allen et al., 2011). The ion channel is a homomeric tetramer, with each subunit having six transmembrane subunits (Keen et al., 1999; Schumacher et al., 2001). During glutamatergic neurotransmission, Ca^{2+} currents driven by NMDAR activity binds to apocalmodulin that is present on SK2 (Lee and MacKinnon, 2018). Ca^{2+} does not directly bind to SK2. However, it activates CaM on SK2 to create conformational changes necessary for the opening of the pore-forming subunits (Kohler et al., 1996; Maylie et al., 2004).

Given that SK2 is calcium activated, an increased activation of NMDAR can promote SK2 activation. Mechanistically, repetitive activation of SK2 promotes K^+ efflux that is necessary for terminating a Ca^{2+} -dependent synaptic potential (Hammond et al., 2006; Lin et al., 2008). Thus, the activity of SK2 may continue to increase until the cell returns to its resting potential (Allen et al., 2007, 2011). The movement of Ca^{2+} and K^+ currents is organized as a synchronous oscillatory process that is dependent on the type of synaptic input and the duration of activation (Fakira et al., 2014). The organization of this process is regulated broadly by CaMKII (which is structurally linked to the GluN2B subunit of NMDAR; Park et al., 2008). During synaptic potentiation, generated Ca^{2+} currents activate CaMKII and consequently facilitate its autophosphorylation at the T286 site. Phosphorylated CaMKII (T286) has a higher affinity for CaM, which increases its activity and affinity for further CaM binding (Dhavan et al., 2002; Coultrap et al., 2014). This process has also been shown to be involved in the modulation of synaptic CaMKII localization in dendritic spines during synaptic potentiation (Coultrap and Bayer, 2012; Coultrap et al., 2014).

Possible Involvement of SK2 and CaMKII in NMDAR Hypofunction

The results of this study showed that both 16p11.2del and Δdisc1 mutations are associated with a significant

upregulation of SK2 in the hippocampus and PFC (Figure 2). Although NMDAR-GluN1 expression was not reduced (Figure 4), it is possible that the upregulation of SK2 in the hippocampus and PFC contributed to the impairment of NMDAR activity in these mutations. This is logical as increased SK2 function can reduce NMDAR potentiation and decrease synaptic Ca^{2+} current (Hammond et al., 2006). In addition to increased SK2 expression, we also found that CaMKII expression was significantly downregulated in both 16p11.2del and Δdisc1 mutation (Figure 3). Furthermore, both 16p11.2del and Δdisc1 mutant mice exhibited a significant impairment of T286 phosphorylation of CaMKII. Together, these outcomes suggest that a state of NMDAR hypofunction in the hippocampus and PFC of 16p11.2del and Δdisc1 mutant mice involves the dysregulation of ion channel and kinase gating of NMDAR activity. These changes were also associated with socio-cognitive defects. As such, 16p11.2del and Δdisc1 mutant mice did not initiate social exploratory contact with novel mice introduced during sociability and social novelty behavioral tests. In addition, both mutant strains exhibited significantly defective memory index when assessed for object recognition memory.

Given that synaptic potentiation of NMDAR and CaMKII T286 phosphorylation are required for hippocampal–cortical neural encoding, we further determined whether a change in SK2 activity is directly related to the behavioral deficiencies exhibited by the mutant strains. Our results show a significant correlation between upregulated SK2 expression, impaired CaMKII T286 phosphorylation, and prolonged ISI duration (K^+ channel opening). The ISI for 16p11.2del is particularly prominent with constant peaks and absence of valleys. This suggests a persistent activation of SK2 which reduced the frequency of spontaneous spiking in hippocampal CA1 neurons (Figure 5 (d) to (f)) and caused a significant loss of synaptic output (Figure 5(g) and (h)).

Neural Encoding Is Defective in the CA1-DG Neurons

As mentioned previously, CaMKII phosphorylation at the T286 site is central to the tuning of NMDAR and SK2 activity. It is important to note that activation of SK2 occurs during the ISI and constitutes after-hyperpolarization currents that are short-lived (<50 ms). In a previous study, we have demonstrated that pharmacological inhibition of NMDAR was associated with an increased SK2 expression which promoted a prolonged after-hyperpolarization phase in whole-cell patch clamp recordings. Here, we physiologically evaluated the activity of SK2 by measuring the ISI and organization of hippocampal-PFC output rasters *in vivo*. Our results showed that an increase in SK2

expression, coupled with the loss of CaMKII T286 phosphorylation, was linked with an increased ISI in 16p11.2del and Δ disc1 mutant CA1-DG field neurons. The effect of the prolonged ISI was further evident in the pattern of neural encoding for two single units recorded through the same continuous event (channel). Both 16p11.2del and Δ disc1 mutant neurons showed an increased percentage of error per trial in raster alignment.

Summary

Our results show that 16p11.2del and 129S: Δ disc1 mutations are associated with an impairment of T286 phosphorylation of CaMKII. Furthermore, both mutants show a significant upregulation of SK2 expression, which was associated with a prolonged ISI and impairment of neural encoding *in vivo*.

Acknowledgments

This study was supported by LSU-SVM New Investigator startup, CBS Corp and LSU-SVM Corp Grant awarded to OOM.

Declaration of Conflicting Interests

The author(s) declared no potential conflicts of interest with respect to the research, authorship, and/or publication of this article.

Funding

The author(s) received no financial support for the research, authorship, and/or publication of this article.

ORCID iD

Olaekan M. Ogundele  <http://orcid.org/0000-0001-9632-2968>

References

- Allen, D., Bond, C. T., Iujan, R., Ballesteros-Merino, C., Lin, M. T., Wang, K., Klett, N., Watanabe, M., Shigemoto, R., Stackman, R. W., Jr., Maylie, J., & Adelman, J. P. (2011). The SK2-long isoform directs synaptic localization and function of SK2-containing channels. *Nat Neurosci*, *14*, 744–749.
- Allen, D., Fakler, B., Maylie, J., & Adelman, J. P. (2007). Organization and regulation of small conductance Ca²⁺-activated K⁺ channel multiprotein complexes. *J Neurosci*, *27*, 2369–2376.
- Anticevic, A., Gancsos, M., Murray, J. D., Repovs, G., Driesen, N. R., Ennis, D. J., Niciu, M. J., Morgan, P. T., Surti, T. S., Bloch, M. H., Ramani, R., Smith, M. A., Wang, X. J., Krystal, J. H., & Corlett, P. R. (2012). NMDA receptor function in large-scale anticorrelated neural systems with implications for cognition and schizophrenia. *Proc Natl Acad Sci U S A*, *109*, 16720–16725.
- Borrie, S. C., Brems, H., Legius, E., & Bagni, C. (2017). Cognitive dysfunctions in intellectual disabilities: The contributions of the Ras-MAPK and PI3K-AKT-mTOR pathways. *Annu Rev Genomics Hum Genet*, *18*, 115–142.
- Brandon, N. J., Millar, J. K., Korth, C., Sive, H., Singh, K. K., & Sawa, A. (2009). Understanding the role of DISC1 in psychiatric disease and during normal development. *J Neurosci*, *29*, 12768–12775.
- Chechlacz, M., & Gleeson, J. G. (2003). Is mental retardation a defect of synapse structure and function? *Pediatr Neurol*, *29*, 11–17.
- Cohen, S. M., Tsien, R. W., Goff, D. C., & Halassa, M. M. (2015). The impact of NMDA receptor hypofunction on GABAergic neurons in the pathophysiology of schizophrenia. *Schizophr Res*, *167*, 98–107.
- Corriveau, R. A., Huh, G. S., & Shatz, C. J. (1998). Regulation of class I MHC gene expression in the developing and mature CNS by neural activity. *Neuron*, *21*, 505–520.
- Coultrap, S. J., & Bayer, K. U. (2012). CaMKII regulation in information processing and storage. *Trends Neurosci*, *35*, 607–618.
- Coultrap, S. J., Freund, R. K., O'Leary, H., Sanderson, J. L., Roche, K. W., Dell'acqua, M. L., & Bayer, K. U. (2014). Autonomous CaMKII mediates both LTP and LTD using a mechanism for differential substrate site selection. *Cell Rep*, *6*, 431–437.
- Crabtree, G. W., Sun, Z., Kvaajo, M., Broek, J. A., Fenelon, K., Mckellar, H., Xiao, L., Xu, B., Bahn, S., O'Donnell, J. M., & Gogos, J. A. (2017). Alteration of neuronal excitability and short-term synaptic plasticity in the prefrontal cortex of a mouse model of mental illness. *J Neurosci*, *37*, 4158–4180.
- Cutsuridis, V., Cobb, S., & Graham, B. P. (2010). Encoding and retrieval in a model of the hippocampal CA1 microcircuit. *Hippocampus*, *20*, 423–446.
- Decker, H., Lo, K. Y., Unger, S. M., Ferreira, S. T., & Silverman, M. A. (2010). Amyloid-beta peptide oligomers disrupt axonal transport through an NMDA receptor-dependent mechanism that is mediated by glycogen synthase kinase 3beta in primary cultured hippocampal neurons. *J Neurosci*, *30*, 9166–9171.
- Dhavan, R., Greer, P. L., Morabito, M. A., Orlando, L. R., & Tsai, L. H. (2002). The cyclin-dependent kinase 5 activators p35 and p39 interact with the alpha-subunit of Ca²⁺/calmodulin-dependent protein kinase II and alpha-actinin-1 in a calcium-dependent manner. *J Neurosci*, *22*, 7879–7891.
- Dibue, M., Kamp, M. A., Alpdogan, S., Tevoufouet, E. E., Neiss, W. F., Hescheler, J., & Schneider, T. (2013). Cav 2.3 (R-type) calcium channels are critical for mediating anti-convulsive and neuroprotective properties of lamotrigine *in vivo*. *Epilepsia*, *54*, 1542–1550.
- Dibue-Adjei, M., Kamp, M. A., Alpdogan, S., Tevoufouet, E. E., Neiss, W. F., Hescheler, J., & Schneider, T. (2017). Cav2.3 (R-type) calcium channels are critical for mediating anticonvulsive and neuroprotective properties of lamotrigine *in vivo*. *Cell Physiol Biochem*, *44*, 935–947.
- Dittrich, L., Petese, A., & Jackson, W. S. (2017). The natural Disc1-deletion present in several inbred mouse strains does not affect sleep. *Sci Rep*, *7*, 5665.

- Eichenbaum, H. (2000). A cortical-hippocampal system for declarative memory. *Nat Rev Neurosci*, *1*, 41–50.
- Fakira, A. K., Portugal, G. S., Carusillo, B., Melyan, Z., & Moron, J. A. (2014). Increased small conductance calcium-activated potassium type 2 channel-mediated negative feedback on N-methyl-D-aspartate receptors impairs synaptic plasticity following context-dependent sensitization to morphine. *Biol Psychiatry*, *75*, 105–114.
- Gandal, M. J., Anderson, R. L., Billingslea, E. N., Carlson, G. C., Roberts, T. P., & Siegel, S. J. (2012). Mice with reduced NMDA receptor expression: More consistent with autism than schizophrenia? *Genes Brain Behav*, *11*, 740–750.
- Gao, J., Stevenson, T. J., Douglass, A. D., Barrios, J. P., & Bonkowsky, J. L. (2018). The midline axon crossing decision is regulated through an activity-dependent mechanism by the NMDA receptor. *eNeuro*, *5*.
- Gao, M., & Zhao, L. R. (2018). Turning death to growth: Hematopoietic growth factors promote neurite outgrowth through MEK/ERK/p53 pathway. *Mol Neurobiol*, *55*, 5913–5925.
- Giese, K. P., Fedorov, N. B., Filipkowski, R. K., & Silva, A. J. (1998). Autophosphorylation at Thr286 of the alpha calcium-calmodulin kinase II in LTP and learning. *Science*, *279*, 870–873.
- Godsil, B. P., Kiss, J. P., Spedding, M., & Jay, T. M. (2013). The hippocampal-prefrontal pathway: The weak link in psychiatric disorders? *Eur Neuropsychopharmacol*, *23*, 1165–1181.
- Gonzalez Burgos, I., Nikonenko, I., & Korz, V. (2012). Dendritic spine plasticity and cognition. *Neural Plast*, *2012*, 875156.
- Halene, T. B., Ehrlichman, R. S., Liang, Y., Christian, E. P., Jonak, G. J., Gur, T. L., Blendy, J. A., Dow, H. C., Brodtkin, E. S., Schneider, F., Gur, R. C., & Siegel, S. J. (2009). Assessment of NMDA receptor NR1 subunit hypofunction in mice as a model for schizophrenia. *Genes Brain Behav*, *8*, 661–675.
- Hammond, R. S., Bond, C. T., Strassmaier, T., Ngo-Anh, T. J., Adelman, J. P., Maylie, J., & Stackman, R. W. (2006). Small-conductance Ca²⁺-activated K⁺ channel type 2 (SK2) modulates hippocampal learning, memory, and synaptic plasticity. *J Neurosci*, *26*, 1844–1853.
- Horev, G., Ellegood, J., Lerch, J. P., Son, Y. E., Muthuswamy, L., Vogel, H., Krieger, A. M., Buja, A., Henkelman, R. M., Wigler, M., & Mills, A. A. (2011). Dosage-dependent phenotypes in models of 16p11.2 lesions found in autism. *Proc Natl Acad Sci U S A*, *108*, 17076–17081.
- Incontro, S., Diaz-Alonso, J., Iafraji, J., Vieira, M., Asensio, C. S., Sohal, V. S., Roche, K. W., Bender, K. J., & Nicoll, R. A. (2018). The CaMKII/NMDA receptor complex controls hippocampal synaptic transmission by kinase-dependent and independent mechanisms. *Nat Commun*, *9*, 2069.
- Keen, J. E., Khawaled, R., Farrens, D. L., Neelands, T., Rivard, A., Bond, C. T., Janowsky, A., Fakler, B., Adelman, J. P., & Maylie, J. (1999). Domains responsible for constitutive and Ca(2+)-dependent interactions between calmodulin and small conductance Ca(2+)-activated potassium channels. *J Neurosci*, *19*, 8830–8838.
- Kohler, M., Hirschberg, B., Bond, C. T., Kinzie, J. M., Marrion, N. V., Maylie, J., & Adelman, J. P. (1996). Small-conductance, calcium-activated potassium channels from mammalian brain. *Science*, *273*, 1709–1714.
- Kvajo, M., Mckellar, H., Arguello, P. A., Drew, L. J., Moore, H., Macdermott, A. B., Karayiorgou, M., & Gogos, J. A. (2008). A mutation in mouse Discl1 that models a schizophrenia risk allele leads to specific alterations in neuronal architecture and cognition. *Proc Natl Acad Sci USA*, *105*, 7076–7081.
- Lee, C. H., & Mackinnon, R. (2018). Activation mechanism of a human SK-calmodulin channel complex elucidated by cryo-EM structures. *Science*, *360*, 508–513.
- Lee, E. J., Choi, S. Y., & Kim, E. (2015). NMDA receptor dysfunction in autism spectrum disorders. *Curr Opin Pharmacol*, *20*, 8–13.
- Li, B. S., Sun, M. K., Zhang, L., Takahashi, S., Ma, W., Vinade, L., Kulkarni, A. B., Brady, R. O., & Pant, H. C. (2001). Regulation of NMDA receptors by cyclin-dependent kinase-5. *Proc Natl Acad Sci U S A*, *98*, 12742–12747.
- Lin, M. T., Lujan, R., Watanabe, M., Adelman, J. P., & Maylie, J. (2008). SK2 channel plasticity contributes to LTP at Schaffer collateral-CA1 synapses. *Nat Neurosci*, *11*, 170–177.
- Lisman, J., Schulman, H., & Cline, H. (2002). The molecular basis of CaMKII function in synaptic and behavioural memory. *Nat Rev Neurosci*, *3*, 175–190.
- Lisman, J., Yasuda, R., & Raghavachari, S. (2012). Mechanisms of CaMKII action in long-term potentiation. *Nat Rev Neurosci*, *13*, 169–182.
- Lovinger, D. M., Colley, P. A., Akers, R. F., Nelson, R. B., & Routtenberg, A. (1986). Direct relation of long-term synaptic potentiation to phosphorylation of membrane protein F1, a substrate for membrane protein kinase C. *Brain Res*, *399*, 205–211.
- Mao, Y., Ge, X., Frank, C. L., Madison, J. M., Koehler, A. N., Doud, M. K., Tassa, C., Berry, E. M., Soda, T., Singh, K. K., Biechele, T., Petryshen, T. L., Moon, R. T., Haggarty, S. J., & Tsai, L. H. (2009). Disrupted in schizophrenia 1 regulates neuronal progenitor proliferation via modulation of GSK3beta/beta-catenin signaling. *Cell*, *136*, 1017–1031.
- Matsuo, N., Yamasaki, N., Ohira, K., Takao, K., Toyama, K., Eguchi, M., Yamaguchi, S., & Miyakawa, T. (2009). Neural activity changes underlying the working memory deficit in alpha-CaMKII heterozygous knockout mice. *Front Behav Neurosci*, *3*, 20.
- Maylie, J., Bond, C. T., Herson, P. S., Lee, W. S., & Adelman, J. P. (2004). Small conductance Ca²⁺-activated K⁺ channels and calmodulin. *J Physiol*, *554*, 255–261.
- Morishita, W., Connor, J. H., Xia, H., Quinlan, E. M., Shenolikar, S., & Malenka, R. C. (2001). Regulation of synaptic strength by protein phosphatase 1. *Neuron*, *32*, 1133–1148.
- Nakazawa, K., Jeevakumar, V., & Nakao, K. (2017). Spatial and temporal boundaries of NMDA receptor hypofunction leading to schizophrenia. *NPJ Schizophr*, *3*, 7.
- Ogundele, O. M., & Lee, C. C. (2018). CaMKIIalpha expression in a mouse model of NMDAR hypofunction schizophrenia: Putative roles for IGF-1R and TLR4. *Brain Res Bull*, *137*, 53–70.

- Parent, M. A., Wang, L., Su, J., Netoff, T., & Yuan, L. L. (2010). Identification of the hippocampal input to medial prefrontal cortex in vitro. *Cereb Cortex*, *20*, 393–403.
- Park, C. S., Elgersma, Y., Grant, S. G., & Morrison, J. H. (2008). Alpha-isoform of calcium-calmodulin-dependent protein kinase II and postsynaptic density protein 95 differentially regulate synaptic expression of NR2A- and NR2B-containing N-methyl-d-aspartate receptors in hippocampus. *Neuroscience*, *151*, 43–55.
- Penzes, P., Cahill, M. E., Jones, K. A., Vanleeuwen, J. E., & Woolfrey, K. M. (2011). Dendritic spine pathology in neuropsychiatric disorders. *Nat Neurosci*, *14*, 285–293.
- Pucilowska, J., Vithayathil, J., Tavares, E. J., Kelly, C., Karlo, J. C., & Landreth, G. E. (2015). The 16p11.2 deletion mouse model of autism exhibits altered cortical progenitor proliferation and brain cytoarchitecture linked to the ERK MAPK pathway. *J Neurosci*, *35*, 3190–3200.
- Ratnadurai-Giridharan, S., Stefanescu, R. A., Khargonekar, P. P., Carney, P. R., & Talathi, S. S. (2014). Genesis of interictal spikes in the CA1: A computational investigation. *Front Neural Circuits*, *8*, 2.
- Reim, D., & Schmeisser, M. J. (2017). Neurotrophic factors in mouse models of autism spectrum disorder: Focus on BDNF and IGF-1. *Adv Anat Embryol Cell Biol*, *224*, 121–134.
- Salter, M. W., & Kalia, L. V. (2004). Src kinases: A hub for NMDA receptor regulation. *Nat Rev Neurosci*, *5*, 317–328.
- Schumacher, M. A., Rivard, A. F., Bachinger, H. P., & Adelman, J. P. (2001). Structure of the gating domain of a Ca²⁺-activated K⁺ channel complexed with Ca²⁺/calmodulin. *Nature*, *410*, 1120–1124.
- Shapiro, M. L., & Eichenbaum, H. (1999). Hippocampus as a memory map: Synaptic plasticity and memory encoding by hippocampal neurons. *Hippocampus*, *9*, 365–384.
- Snyder, M. A., & Gao, W. J. (2013). NMDA hypofunction as a convergence point for progression and symptoms of schizophrenia. *Front Cell Neurosci*, *7*, 31.
- Stein, I. S., Gray, J. A., & Zito, K. (2015). Non-ionotropic NMDA receptor signaling drives activity-induced dendritic spine shrinkage. *J Neurosci*, *35*, 12303–12308.
- Tropea, D., Molinos, I., Petit, E., Bellini, S., Nagakura, I., O’Tuathaigh, C., Schorova, L., Mitchell, K. J., Waddington, J., Sur, M., Gill, M., & Corvin, A. P. (2016). Disrupted in schizophrenia 1 (DISC1) L100P mutants have impaired activity-dependent plasticity in vivo and in vitro. *Transl Psychiatry*, *6*, e712.
- Wang, Q., Charych, E. I., Pulito, V. L., Lee, J. B., Graziane, N. M., Crozier, R. A., Revilla-Sanchez, R., Kelly, M. P., Dunlop, A. J., Murdoch, H., Taylor, N., Xie, Y., Pausch, M., Hayashi-Takagi, A., Ishizuka, K., Seshadri, S., Bates, B., Kariya, K., Sawa, A., Weinberg, R. J., Moss, S. J., Houslay, M. D., Yan, Z., & Brandon, N. J. (2011). The psychiatric disease risk factors DISC1 and TNIK interact to regulate synapse composition and function. *Mol Psychiatry*, *16*, 1006–1023.
- West, A. E., Chen, W. G., Dalva, M. B., Dolmetsch, R. E., Kornhauser, J. M., Shaywitz, A. J., Takasu, M. A., Tao, X., & Greenberg, M. E. (2001). Calcium regulation of neuronal gene expression. *Proc Natl Acad Sci USA*, *98*, 11024–11031.
- Yamasaki, N., Maekawa, M., Kobayashi, K., Kajii, Y., Maeda, J., Soma, M., Takao, K., Tanda, K., Ohira, K., Toyama, K., Kanzaki, K., Fukunaga, K., Sudo, Y., Ichinose, H., Ikeda, M., Iwata, N., Ozaki, N., Suzuki, H., Higuchi, M., Suhara, T., Yuasa, S., & Miyakawa, T. (2008). Alpha-CaMKII deficiency causes immature dentate gyrus, a novel candidate endophenotype of psychiatric disorders. *Mol Brain*, *1*, 6.